Oncogene (2020) 39:3803–3820
https://doi.org/10.1038/s41388-020-1255-y

ARTICLE

Feedback analysis identifies a combination target for overcoming adaptive resistance to targeted cancer therapy

Sang-Min Park[1] · Chae Young Hwang[1] · Jihye Choi[1] · Chang Young Joung[1] · Kwang-Hyun Cho[1]

Received: 22 September 2019 / Revised: 26 February 2020 / Accepted: 28 February 2020 / Published online: 10 March 2020

Abstract

Targeted drugs aim to treat cancer by directly inhibiting oncogene activity or oncogenic pathways, but drug resistance frequently emerges. Due to the intricate dynamics of cancer signaling networks, which contain complex feedback regulations, cancer cells can rewire these networks to adapt to and counter the cytotoxic effects of a drug, thereby limiting the efficacy of targeted therapies. To identify a combinatorial drug target that can overcome such a limitation, we developed a Boolean network simulation and analysis framework and applied this approach to a large-scale signaling network of colorectal cancer with integrated genomic information. We discovered Src as a critical combination drug target that can overcome the adaptive resistance to the targeted inhibition of mitogen-activated protein kinase pathway by blocking the essential feedback regulation responsible for resistance. The proposed framework is generic and can be widely used to identify drug targets that can overcome adaptive resistance to targeted therapies.

Introduction

Although targeted cancer therapy can rapidly reduce tumor burden, persistent clinical responses in patients are rare [1]. As treatment continues, the efficacy of targeted therapy in cancer becomes limited by drug resistance. Therefore, understanding the mechanisms that cause drug resistance is an important challenge to improving cancer treatment. Cellular homeostasis confers drug resistance to cancer cells [2, 3]. Cellular homeostasis is maintained by interacting cellular molecules that form a complex network, which has been evolutionarily designed to be robust to external perturbations, including drugs that affect the molecules in the network. This hardwired homeostatic mechanism, which is intrinsic to the intracellular molecular regulatory network, enables cells to maintain biological functions under suboptimal conditions. Unfortunately, for cancer patients, this homeostatic mechanism also limits the therapeutic effects of treatment. For example, after the treatment with a targeted drug that alters phosphorylation-mediated cellular signaling, dynamic reprogramming of the kinome occurs in the cancer signaling network to adapt and counteract the drug's effect; consequently, cancer cells withstand the drug treatment [4, 5]. This mechanism of drug resistance, which is hard to predict, is referred as "adaptive resistance" [6].

Examples of adaptive resistance involve drugs targeting various kinases in the mitogen-activated protein kinase (MAPK) cascade: RAS → RAF → MEK → ERK. The drug vemurafenib (PLX4032) is an FDA-approved BRAF inhibitor (BRAFi) that is used to treat patients harboring the mutant BRAF V600E. Vemurafenib was effective as a monotherapy in BRAF-mutant melanoma, producing a response rate of 80%; whereas it has failed as a monotherapy in BRAF-mutant colorectal cancer (CRC), producing response rate less than 5% [7]. When the BRAF-mutant CRC was treated with BRAFi, negative feedback from downstream ERK to the upstream receptor EGFR was alleviated [8, 9]. As a result, adaptive resistance emerged against BRAFi through continuous activation of the MAPK signaling pathway by EGFR. In the case of KRAS-mutant

These authors contributed equally: Sang-Min Park, Chae Young Hwang

Supplementary information The online version of this article (https://doi.org/10.1038/s41388-020-1255-y) contains supplementary material, which is available to authorized users.

✉ Kwang-Hyun Cho
ckh@kaist.ac.kr

[1] Laboratory for Systems Biology and Bio-inspired Engineering, Department of Bio and Brain Engineering, Korea Advanced Institute of Science and Technology (KAIST), Daejeon 34141, Republic of Korea

CRC, treatment with an MEK inhibitor (MEKi) induces adaptive resistance that activates the MAPK signaling pathway through BRAF and CRAF [10].

Systems analysis of network dynamics using quantitative mathematical models is an effective method to evaluate and predict the emergence of resistance mechanisms in the complicatedly intertwined signaling network [11–14]. For analyzing a large-scale network, some computational studies have reconstructed and analyzed cancer signaling networks using Boolean models [15, 16]. Signaling molecules are mapped to nodes of a network and the state of a node denotes the activation level of a corresponding molecule. The Boolean model represents the state value of a node in a discrete way ("ON" represented by the value 1 for an active state or "OFF" represented by the value 0 for an inactive state) and represents the dynamics of a node as a logical relationship between nodes. Therefore, the Boolean model is computationally tractable and avoids the problem of parameter estimation, which is necessary for continuous models with ordinary differential equations (ODEs) [17–19]. The effect of drug perturbation for investigating drug responses in Boolean network models is generally implemented by fixing the state value of target node(s) to OFF. Consequently, a signaling pathway can be fully blocked by a single drug targeting one of nodes in the pathway, and adaptive resistance in the pathway cannot be captured by this approach. Therefore, partially inhibited states are required to appropriately represent the drug effect in the simulation and predict mechanisms of adaptive resistance.

Here, we developed a simulation framework that represents drug inhibition as a ratio using a probabilistic Boolean model, and we showed that this approach can capture the adaptive changes that result from changes in feedback regulation after drug treatment. We also reconstructed a comprehensive large-scale signaling network of CRC that encompasses frequently mutated oncogenic pathways with feedback loops and crosstalk paths. By integrating genomic information within the network, we analyzed cell line-specific dynamics in response to targeted inhibitors. To identify combination targets for overcoming adaptive resistance, we evaluated the dynamical change of all the nodes after drug treatment and their feedback composition with respect to the original drug target. We found that Src is an essential target mediating adaptive resistance to multiple drugs targeting the MAPK pathway. Src reactivated the targeted pathway and mediated activation of the compensatory pathway, thereby bypassing the blocked targeted pathway. We experimentally validated that combination treatment of Src inhibitor (SRCi) is effective with MEKi in CRC cell lines (HCT116 and SW620) with mutant KRAS, and with BRAFi or pan-RAF inhibitor (RAFi) in the CRC cell line HT29 with mutant BRAF. Moreover, we confirmed that the combination of SRCi with MAPK pathway inhibitors is effective in lung and breast cancer cells having KRAS or BRAF mutation. The combination of SRCi and phosphatidylinositol-3 kinase (PI3K) pathway inhibitors was also effective in PI3K-mutant CRC cells. Together, we conclude that combinatorial targeting of Src may be effective in preventing adaptive drug resistance in various cancer cells. The proposed simulation framework is generic, so it can be used to identify combinatorial targets for overcoming adaptive resistance of various anticancer drugs.

Results

Development of a Boolean simulation framework to analyze adaptive resistance

We sought to find molecular targets that could inhibit adaptive resistance to drugs in CRC. Treatment of CRC with MAPK signaling pathway inhibitors, such as BRAFi or MEKi, induces adaptive resistance by reactivation of MAPK signaling [8–10]. To establish that this phenomenon occurred in a CRC cell line, we investigated whether BRAFi or MEKi induce the reactivation of their downstream molecule, ERK, in HCT116 and HT29 cells. In the HCT116 cells, treatment with U0126 (MEKi) initially (1 h) reduced the amount of phosphorylated ERK (pERK) levels then pERK amounts recovered by 48 h (Fig. 1a, top). Similarly, in the HT29 cells, treatment with the vemurafenib (BRAFi) initially reduced pERK and then pERK recovered (Fig. 1a, bottom). To illustrate this phenomenon within a network, we created a toy model of the signaling network with a negative feedback loop (NFL). The model network consists of three cascading nodes that convey signals from upstream node A to downstream nodes B and C and an NFL from node C to node A (Fig. 1b (i)). The activity level of output node C indicates the pathway activity. Initially, when node B is targeted by an inhibitor, the drug target node is inhibited and pathway signaling is blocked (Fig. 1b (ii)). However, the reduced activity of downstream node C alleviates its negative feedback to upstream node A and the activated upstream signaling can overcome the inhibitory effect of the drug at node B, enabling the network to adapt and signal transduction to recover (Fig. 1b (iii)). This adaptive change in the network reactivates node B and restores signal transmission through the network in the presence of the inhibitory drug targeting node B (Fig. 1b (iv)). Thus, the NFL enabled the pathway to resist inhibition by drug treatment.

To systematically investigate the effect of feedback regulation using Boolean modeling, we simulated drug treatment in models of the three-node signaling network with or without an NFL (Fig. 1c and Supplementary Table 1). Using a deterministic Boolean network (DBN), the

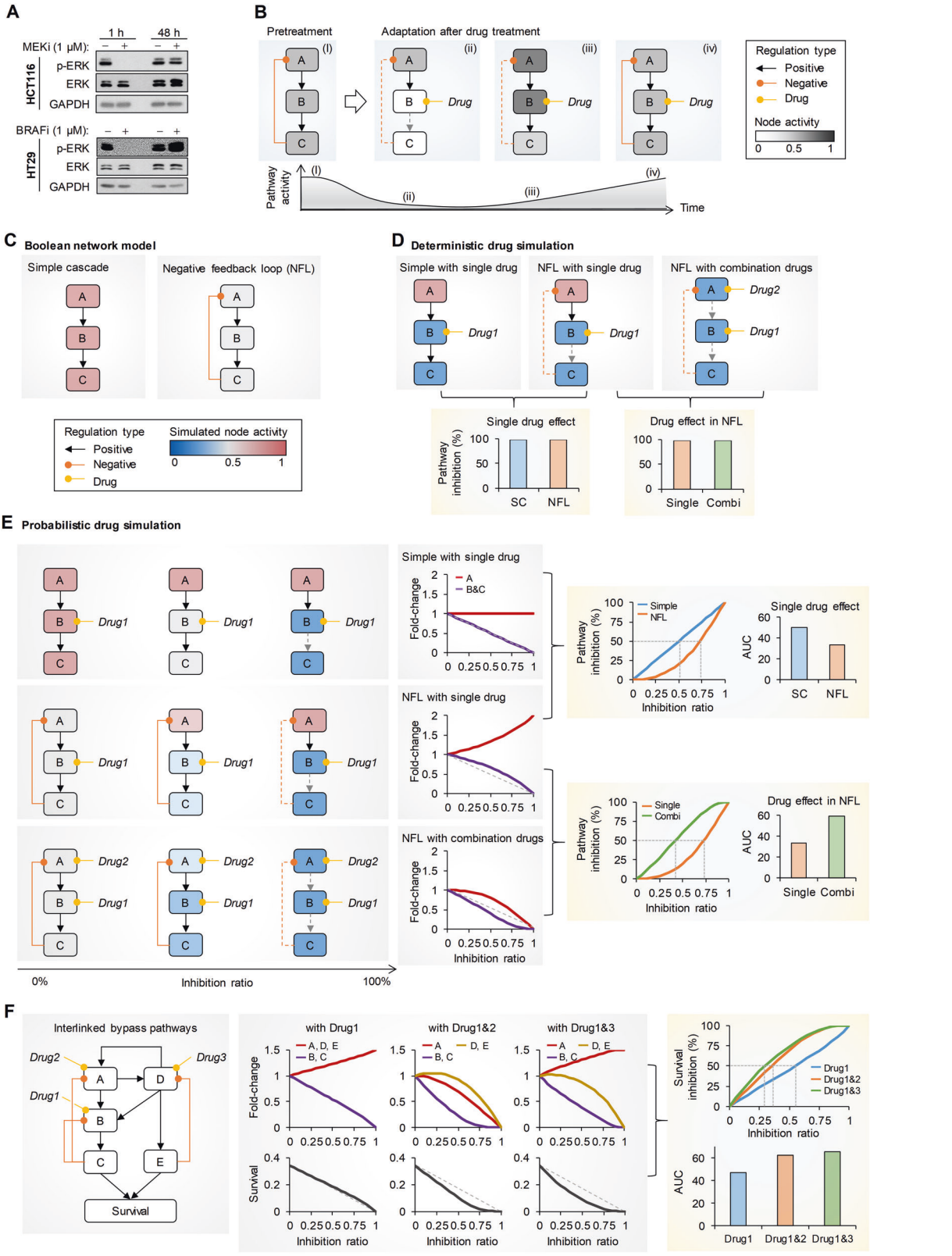

targeted node (node B) is fixed in the OFF state. The deterministic drug simulation resulted in both networks producing the same outcome in the presence of the drug—complete pathway inhibition (Fig. 1d). Furthermore, with the DBN, single and combinatorial drug perturbations to the NFL-containing network produced the same complete

◀ **Fig. 1 Simulation framework to analyze the adaptive resistance to drugs. a** HCT116 or HT29 cells were treated with MEKi (U0126, 1 μM) or BRAFi (vemurafenib, 1 μM). The phosphorylation ERK was monitored for 1 and 48 h by immunoblotting with antibodies recognizing the indicated proteins or phosphoproteins. **b** Illustrative toy model of adaptive resistance in a signaling pathway with negative feedback. The pathway activity was assumed to be the activity of downstream output node C. Each stage of the plotted pathway activity (below) corresponds to a state of the pathway (i, ii, iii, or iv). **c** Boolean network models of a signaling pathway, including three nodes with (NFL) or without negative feedback (simple cascade). **d** The results obtained by deterministic drug simulation of the response to one or two drugs. **e** The results obtained by the probabilistic drug simulation of the response to one or two drugs. Simulated node activity in **c**, **d**, and **e** is represented by the blue to red scale below in **c**. **f** The Boolean network model of the signaling pathway with interlinked bypass pathways and the results obtained by the probabilistic drug simulation.

inhibition of the pathway (Fig. 1d), which is not reflective of the experimentally identified effectiveness of this combination in inhibiting the MAPK pathway [10, 20]. Thus, the conventional approach with deterministic drug simulation based on a binary response cannot effectively represent adaptive resistance that arises from an NFL and thus cannot identify combinatorial targets.

To overcome this limitation, we developed a Boolean simulation framework, which we call probabilistic Boolean modeling with a probabilistic Boolean network (PBN), for the analysis of adaptive resistance in a signaling network by incorporating an inhibition ratio for the drug target nodes. The incorporation of an inhibition ratio is more reflective of the in vivo situation where a drug is unlikely to block 100% of a protein's function. In contrast to a DBN in which the state of a node in the network is updated by one logic during the simulation, a PBN incorporates uncertainty such that the state of a node in the PBN is stochastically updated according to one of several logics [21]. In our probabilistic Boolean modeling, a drug target node has two Boolean functions, the original and inhibitory logics (Supplementary Fig. 1). We chose the inhibitory logic for the drug target node with a probability of the inhibition ratio. As a result, the state value of the drug target node was probabilistically inhibited according to the inhibition ratio in the range from 0 to 1. If a drug target node was inhibited with the ratio of 30%, the state of the target node was fixed to OFF in 30% simulation steps following the inhibitory logic and was continuously updated following the original logic of the node in the remaining simulation steps (70%).

By the probabilistic drug simulation, we captured the emergence of drug resistance in an NFL-containing network compared the absence of resistance in simple cascade (Fig. 1e, left panel). The simple cascade exhibited an inhibition of pathway activity linearly correlated with the inhibition ratio without any changes in the activity of the node upstream of the drug target node; the NFL network exhibited an increase in the activity of the node upstream of the drug target node and the block of pathway activity was slowly achieved with the inhibition ratio (Fig. 1e, middle panel). Inhibition of the NFL network developed at higher amount of the inhibition ratio than that required to inhibit the simple cascade. By combinatorial drug targeting the node A, inhibition of the NFL network occurred at lower amounts of inhibition ratio than those required by the single drug, indicating more effective inhibition of pathway activity by the combinatorial targeting of node A and node B. The area under curve (AUC) for the pathway inhibition of the PBN clearly demonstrated the resistance of the NFL network and the enhanced effect of drug combination (Fig. 1e, right panel), compared with those results of the DBN (Fig. 1d, bottom). This analysis demonstrated that our simulation framework using PBN can represent NFL-mediated adaptive resistance and thus can identify combinatorial targets to overcome resistance mediated by feedback regulation.

We tested our simulation framework in a model of the more complicated toy model with interlinked bypass pathways, including multiple negative and positive feedback loops (Fig. 1f, left panel and Supplementary Table 1). Node D in this model can contribute to pathway activity through multiple bypass routes. Intriguingly, node D, rather than A, was the most effective combinatorial target with node B in this model (Fig. 1f, middle and right panel). This result was also demonstrated in the toy model with different logical function (Supplementary Fig. 2). Considering that node D is outside the pathway from A–B–C pathway initially, this result suggested that combination targets may be outside the initially targeted pathway and thus would be difficult to predict without a computational approach. It is noteworthy that the results of deterministic drug simulation (at 100% inhibition ratio) could not predict effects of single and combination drugs, as well as of different combinatorial targets.

Reconstruction of the large-scale signaling network for CRC

Because the signaling network common in many cancer cells contains numerous feedback regulations and crosstalk among multiple modular pathways [3], the mechanism of adaptive resistance to drugs may not be intuitive or readily predictable. To systematically analyze mechanism of the adaptive resistance to drugs in CRC, we reconstructed a Boolean model for a large-scale comprehensive signaling network of CRC based on the published literature and information in such databases as Pathway Interaction Database and Kyoto Encyclopedia of Genes and Genomes (KEGG) [22, 23]. Within the signaling pathways, we integrated frequently mutated components associated with

colorectal tumorigenesis [24, 25], including APC or β-catenin mutations in the WNT pathway, BRAF or KRAS mutations in the MAPK pathway, PI3Kα mutations in the PI3K/AKT pathway, SMAD4 mutations in the TGFβ pathway, p53 mutations in the DNA damage pathway, and we included crosstalk links between pathways. We also included pathways that represented the outcome of the drug response: p38/JNK pathway, JAK/STAT pathway, cell cycle pathway, and apoptosis pathway. The entire signaling network of CRC consists of 95 nodes and 341 links (Fig. 2a and Supplementary Data 1 for logic equations). Four input nodes (EGF, DNA damage, WNT, and TGFβ) stimulate the corresponding signaling pathways of the network model. Two output nodes (proliferation and apoptosis) represent the phenotypes produced by the network model.

We note that most isoforms are represented as a single node in this network, for instance, both ERK1 and ERK2 are incorporated as an ERK node, except RAF that different roles of its isoforms are demonstrated experimentally as critical in adaptive resistance. CRAF was revealed to be activated for the reactivation of MAPK pathway against BRAFi in BRAF-mutant CRC cells [9]. If BRAF and CRAF are combined and represented by a single node (RAF), such a reactivation mechanism cannot be analyzed. Thus, we modeled BRAF and CRAF as separate nodes with the same regulatory logics in our signaling network. Only BRAF node was affected by BRAF mutation or inhibition while CRAF node was intact in our simulations.

To investigate the dynamics of this CRC signaling network without any genetic alterations, we performed qualitative simulations with different levels of inputs from 0 to 100%. If the level of an input was 30%, the state of the input node was fixed to ON in 30% simulation steps or OFF in the other 70%. The results showed that our network model reproduced relevant input–output relationships of the signaling network (Fig. 2b and Supplementary Table 2). EGF stimulation exhibited a positive relationship with the activity of ERK, AKT, S6K, c-MYC, and CyclinD, and negative relationship with the activity of p27 [26]. DNA damage stimulation exhibited a positive relationship with the activity of p53 and p21 [27]. WNT stimulation exhibited a positive relationship with the activity of β-catenin, c-MYC, and CyclinD [28]. TGFβ stimulation exhibited a positive relationship with the activity of Smad4 (combined with Smad2/3), ERK, and AKT [29].

We next generated cell line-specific signaling networks for CRC using genomic information The Cancer Cell Line Encyclopedia (CCLE) [30]. Among the genetic alterations of 60 CRC cell lines, we selected those producing functional oncogenic mutations that mapped onto our signaling network. The effect of the genetic alteration was categorized as either the gain of function or the loss of function according to OncoKB database [31], such that each genetic alteration was mapped onto the network by a binary way: activated (fixed as ON) or inactivated (fixed as OFF). The result was 37 differentially wired CRC networks (Fig. 3).

Identification of combinatorial drug target for overcoming adaptive resistance

To verify our simulation framework in cell line-specific signaling networks of CRC, we compared the simulation results of drug perturbations with those reported for published experiments. In the literature, combination of MEKi and RAFi suppressed ERK reactivation in KRAS-mutant CRC cells (SW480) [10]. Similarly, this combination was more effective in suppressing ERK activity in our simulations of the corresponding CRC network (Supplementary Fig. 3A). BRAFi caused ERK reactivation by EGFR via CRAF in BRAF-mutant CRC cells (HT29, LS411N, and SW1417) [9], and our simulation reproduced this adaptive response and combination effect with EGFRi in the corresponding CRC networks (Supplementary Fig. 3B).

To identify effective combination targets for an MAPK inhibitor in our network model, we attempted to develop a scoring system in target prediction metrics based on the network mechanism for adaptive resistance. We expected that critical nodes for adaptive resistance would show a high amount of activity change (AC) after drug treatment, be connected with a short NFL, transmit more positive bypass signals to proliferation node, and transmit more negative bypass signals to apoptosis node. The score was formulated based on three criteria that take into account both network dynamics and structure (Fig. 4a; and see "Methods"): changes in node activity after drug treatment, strength of the negative feedback, and the presence of bypass signaling. We evaluated the change in the activity of candidate nodes after the drug treatment, because a high increase in the activity of a node upstream of the drug target node may strongly contribute to pathway reactivation. We evaluated feedback strength of candidate nodes as the activity changes divided by the lengths of shortest NFLs between ERK and candidate nodes, because the signaling effect of longer pathways may be attenuated relative to shorter pathways due to competition among signaling molecules and feedback structure with shorter length may be more functional in adaptive resistance [32]. We evaluated the bypass signaling effects from candidate nodes to cell survival and apoptosis pathways, because these may also confer drug resistance.

Based on the scores obtained from MEKi simulations of the HCT116 and SW620 networks, and BRAFi simulation of the HT29, upstream nodes such as EGFR and IGFR was identified as effective targets in agreement with previous experiments [33, 34] (Fig. 4b and Supplementary Data 2). However, the most effective candidate target to overcome

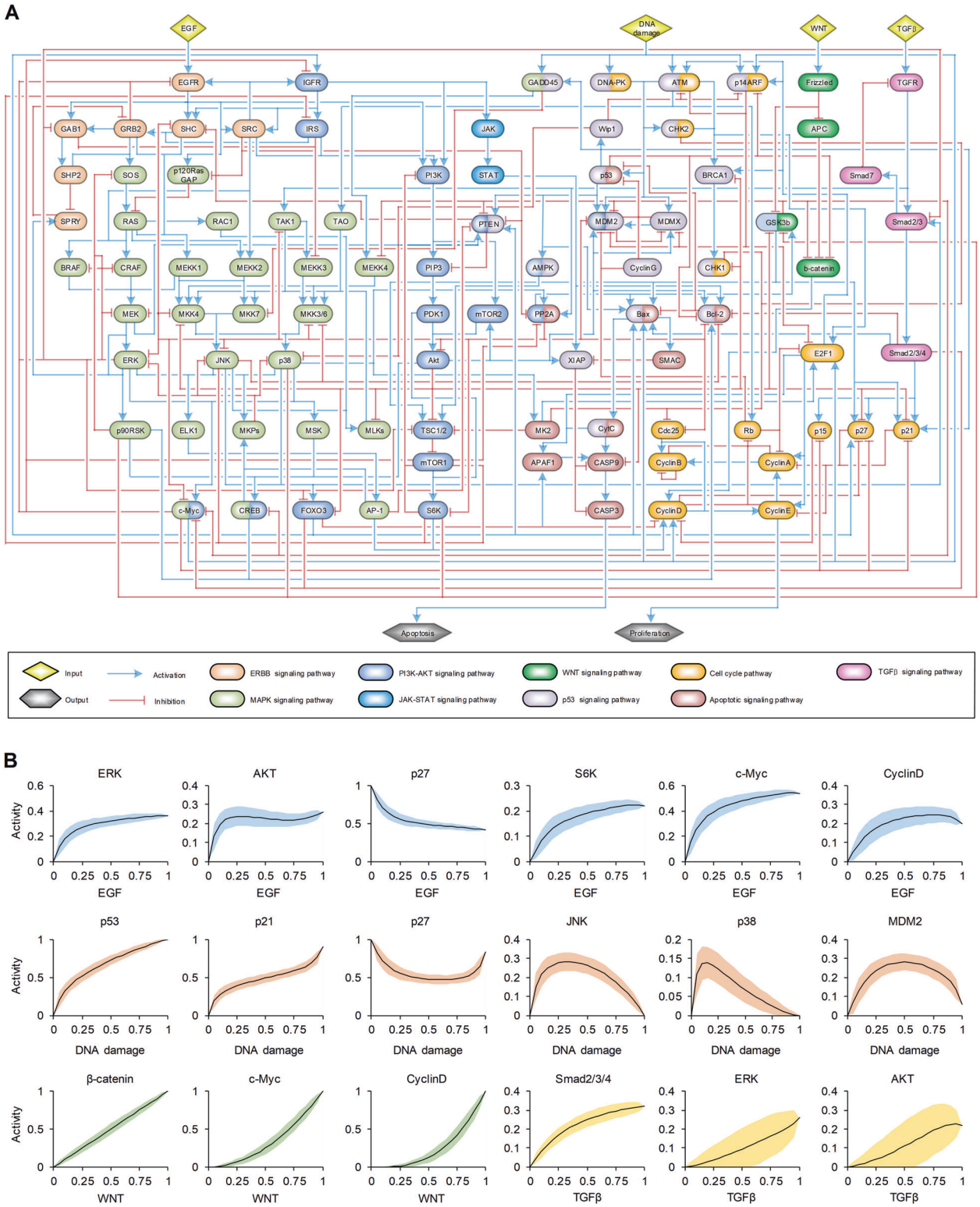

Fig. 2 Reconstruction of a large-scale signaling network of CRC. **a** The reconstructed CRC signaling network is composed of 95 nodes and 341 links. This network includes four input nodes and two phenotypic output nodes. The colors of other nodes indicate the corresponding KEGG pathways. The links are classified as activation with a blue arrow line or inhibition with a red blunted line. **b** Responses of the network model to stimulation of input nodes: EGF, DNA damage, WNT, or TGFβ. The stimulation level by the input nodes was varied in the range of 0–100% representing the average ratio of the ON state during the simulation time. The activity of downstream nodes was measured by average ratio of the ON state during the simulation time.

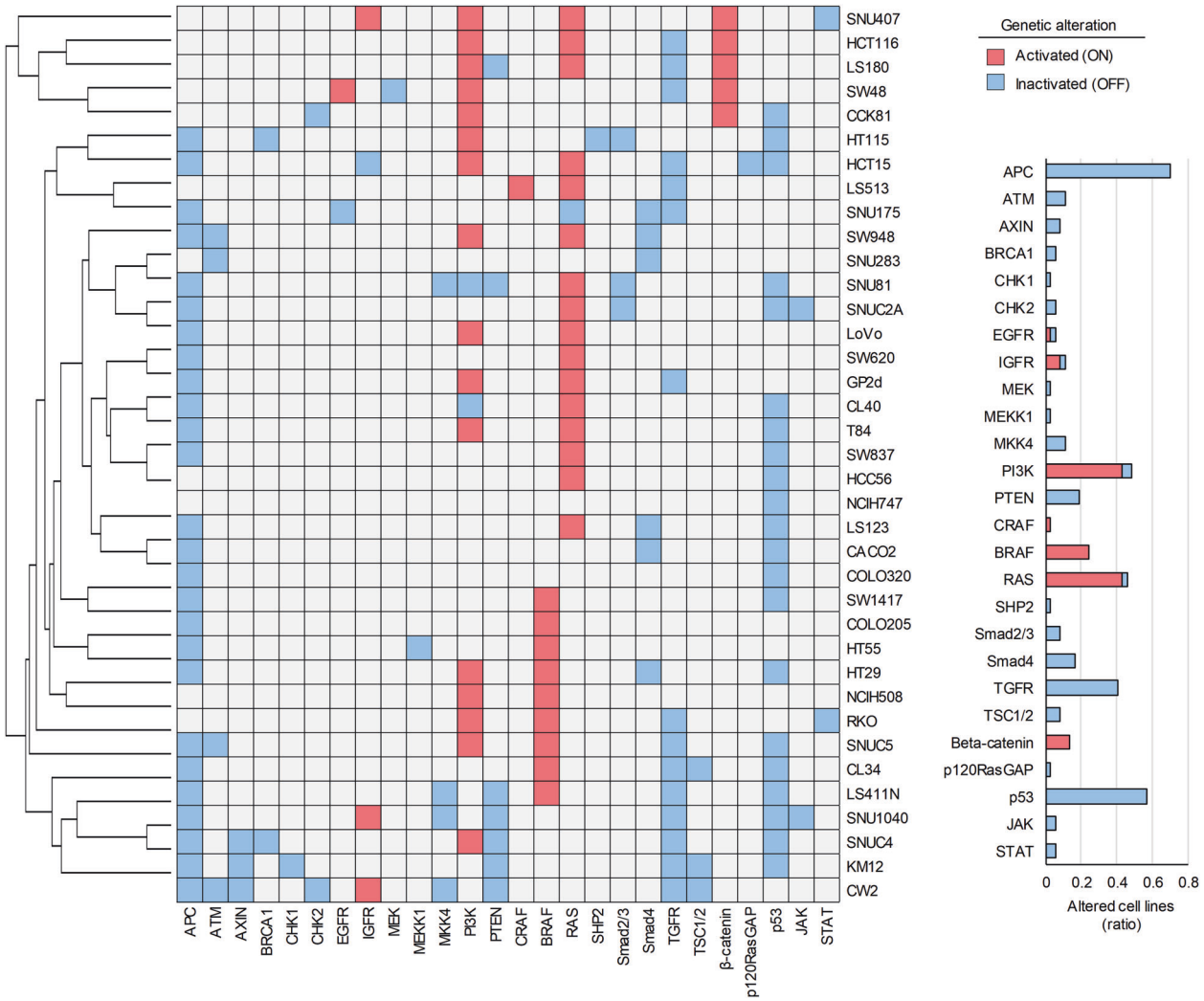

Fig. 3 Mapping genomic information to cell line-specific CRC networks. The 37 differentially wired networks were generated by integrating genomic information into the reconstructed signaling network from CCLE database. The effect of the genetic alteration on the corresponding node in the network was classified as constantly activated (ON) or inactivated (OFF) state depending on the oncogenic function of the alteration. Mapped networks were sorted by hierarchical clustering (left). The ratio of genetic alteration for each node among the 37 networks was plotted (right).

the resistance of MAPK pathway inhibitors was Src in those cell networks. The scores for every node were obtained from the simulations of 37 cell line-specific signaling networks, which predicted that Src is commonly found as the best combination target with MAPK pathway inhibitors in CRC cell lines, followed by EGFR, CRaf, and Akt (Supplementary Data 3). This result was supported by extensive simulations for inhibiting every node in combination with initial drug treatments using MEKi for HCT116 and SW620 networks or BRAFi for HT29 network (Supplementary Data 4). By evaluating activity changes of ERK, apoptosis, and proliferation nodes from the simulation results, the most effective combinatorial target was Src as predicted by the score (Supplementary Fig. 4).

Src has a complex interaction with the MAPK pathway in our network model (Fig. 4c). It would be noteworthy that this network seems to be similar to the toy model of interlinked bypass pathways (Fig. 1f, left). The role of Src in the network corresponds to node D in the toy model of which combinatorial inhibition is effective to suppress the signaling. This suggests that inhibition of Src can cooperate with the MAPK pathway inhibitors. Since Src participates in positive feedback with upstream receptors that is increased after treatment with MAPK pathway inhibitors, Src can reinforce the adaptive activation of upstream signaling. Activated Src can also directly stimulate the MAPK pathway though a crosstalk with RAF to confer the pathway reactivation. In addition, Src can activate a bypass pathway through other survival pathways and eventually produce drug resistance. Therefore, Src may function as a resistance hub against the response to MAPK pathway inhibitors. To predict the effect of drug combination in the CRC signaling

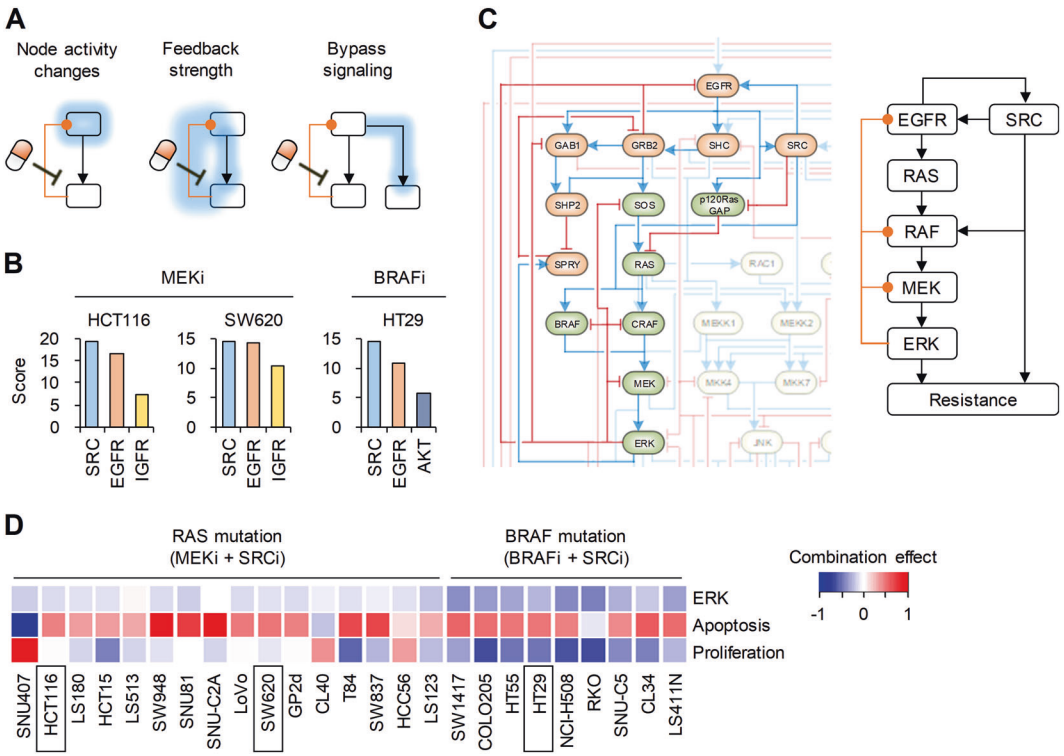

Fig. 4 Identification of combinatorial targets for overcoming adaptive resistance. a Three criteria for identifying a combinatorial target from candidate nodes: change in the activity of a candidate node, the strength of the feedback loop between ERK and a candidate node, and the effect of bypass signaling of a candidate node on proliferation and apoptosis. **b** Top three scores of candidate combinatorial targets for MEKi in the HCT116 (left) and SW620 networks (middle), and BRAFi in the HT29 network (right). **c** Simplified network of the interactions between Src and the MAPK pathway (right) extracted from the CRC signaling network (left). **d** The simulation results for drug combination of SRCi with MEKi or BRAFi in the cell line-specific networks with activated RAS or BRAF mutations, respectively. The combination effect on ERK node was evaluated as the difference between the activity change of combined drug treatments and the maximum activity change of single drug treatments. The combination effects on proliferation and apoptosis nodes were evaluated as the difference between the activity change of combined drug treatments and the summed activity change of single drug treatments. The cell line names with a rectangle were used for further experimental validations.

network, the drug combination effects on the activities of ERK and the output nodes, proliferation, and apoptosis, were evaluated against the effects of single drug treatments. Consistent with our hypothesis, the simulation results showed that combination treatment with SRCi and MAPK pathway inhibitors was effective in suppressing MAPK pathway activity, as well as decreasing cell proliferation and increasing apoptosis (Fig. 4d). Thus, we thought that SRCi can broadly sensitize the responsiveness of MEKi or BRAFi in KRAS- or BRAF-mutant CRC cells, respectively.

Empirical testing of the combination of an Src inhibitor with an MAPK pathway inhibitor in CRC cells

To examine whether combinatorial treatment with an SRCi and an MAPK pathway inhibitor prevented resistance to the MAPK pathway inhibitor in CRC cell lines, we used dasatinib as the SRCi, trametinib as the MEKi, vemurafenib as the BRAFi, and AZ628 as an RAFi in CRC cells with KRAS mutations (HCT116 and SW620 cells) and cells with a BRAF mutation (HT29 cells) (Supplementary Table 3).

The simulations of the HCT116 network (KRAS G13D and PI3K H1047R mutations) showed that the combination of SRCi with MEKi suppressed SRC activation induced by MEKi, slightly reduced the activities of ERK and proliferation nodes, and effectively increased the activity of apoptosis node (Figs. 4d and 5a). In the experiments with these cells, we exposed the cells to trametinib alone, dasatinib alone, or their combination for 3 days. We monitored cell confluence (Fig. 5b), viability (Fig. 5c), colony formation (Fig. 5d), activity of ERK and SRC (amount of their phosphorylated forms by Western blot) (Fig. 5e), and apoptosis by flow cytometry analysis (Fig. 5f, g). The combination of trametinib and dasatinib had a synergistic inhibitory effect in the viability of HCT116 cells (Fig. 5b, c). In addition, crystal violet assays and phase contrast images also confirmed the synergistic effect (Fig. 5d). Consistent with our expectations, HCT116 cells exposed to trametinib exhibited a transient reduction in pERK 1 h after

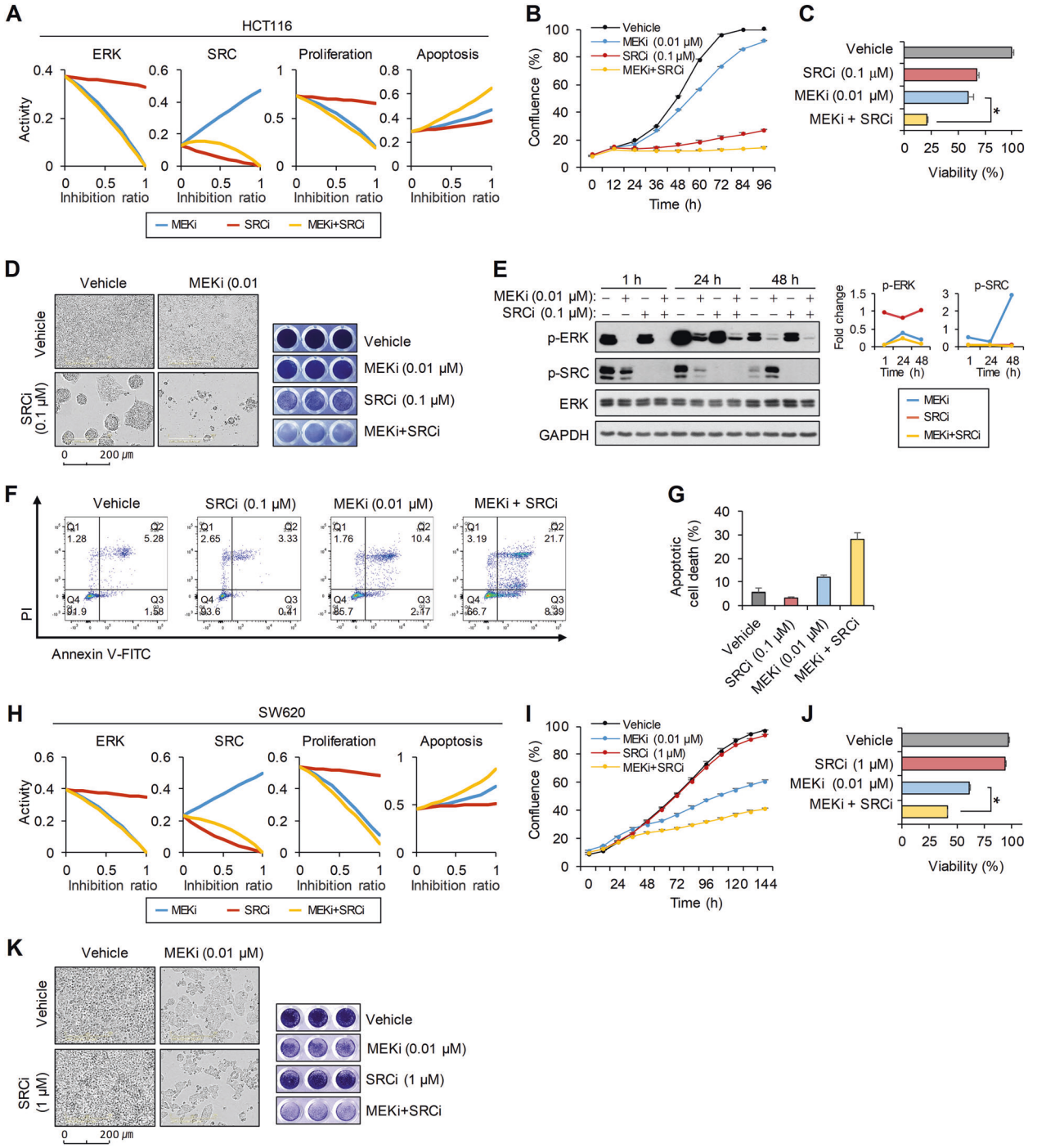

exposure, and this was followed by a rebound in its activity after 24 h (Fig. 5e). In contrast, SRCi alone had little effect on pERK abundance, but the combination of trametinib and dasatinib limited the rebound in ERK activity after 24 h. Furthermore, as predicted in our simulations, the combination treatment of MEKi and SRCi significantly increased early (PI^-, FITC-annexin V^+) and late (PI^+, FITC-annexin V^+) cell death compared with those cells treated with MEKi alone or SRCi alone in HCT116 cells (Fig. 5f, g). The simulations of the SW620 network, which has KRAS G12V mutation without PI3K mutation, also showed combinatorial effect of SRCi and MEKi (Figs. 4d and 5h). In this cell line, SRCi alone had less of an inhibitory effect on viability than SRCi alone had on HCT116 cells (compare Fig. 5b and Fig. 5i, and Fig. 5c and Fig. 5j). However, like the HCT116 cells, the combination of dasatinib and trametinib was synergistic in reducing cell viability (Fig. 5i–k).

◀ **Fig. 5 Combination effect of SRCi and MEKi in KRAS-mutant CRC cells. a** Simulated drug response curves in the HCT116 network. **b** Analysis of cell growth. HCT116 cells were incubated for 24 h in 96-well plate (0.7×10^4 cells/well) and then treated with MEKi (trametinib, 0.01 μM) alone, SRCi (dasatinib, 0.1 μM) alone, or in combination for 3 days. Cell growth was determined by cell confluence (%). **c** Analysis of cell viability. Cell viability was determined by the WST-1 assay after 3 days treatment with indicated drugs. **d** Images were taken 3 days after the indicated treatments (left). Crystal violet staining of colony growth treated with indicated drugs (right). **e** HCT116 cells were subjected to the indicated treatments, then the indicated proteins were detected by Western blot. pERK is an indicator of adaptive resistance. pERK and p-SRC were quantified and normalized with GAPDH. Line graphs were plotted by fold change values normalized with vehicle at each time point. **f** Apoptotic cell death of HCT116 cells. Cells were treated with the MEKi (0.01 μM), SRCi (0.1 μM), and MEKi plus SRCi for 48 h. Cells were stained with PI and Annexin V-FITC, and were analyzed by flow cytometry (Q4: live cells; Q3: early apoptotic cells; Q2: late apoptotic cells; Q1: necrotic cells). The acquisition of Annexin V-FITC and PI data is expressed as a percentage (%) in each quadrant. **g** The percentage of apoptotic cell death was examined by annexin V-FITC/PI staining and flow cytometry analysis. The results are presented as mean ± SD of two independent experiments. **h** Simulated drug response curves in the SW620 network. **i** Analysis of cell growth. SW620 cells were treated with MEKi (trametinib, 0.01 μM) alone, SRCi (dasatinib, 1 μM) alone, or in combination for 5 days. Cell growth was determined by cell confluence (%). **j** Analysis of cell viability. Cell viability was determined by WST-1 assay after 5 days treatment with indicated drugs. **k** Images of SW620 cells were taken 5 days after the indicated treatments (left). Crystal violet staining of colony growth treated with indicated drugs (right). The results are presented by means ± SEM (error bars) ($n = 3$). $^*P < 0.05$ by two-sided Student's t test.

To determine if this synergistic response was also observed with cells with a mutation at a different point in the MAPK pathway and with drugs targeting that mutated node, we examined the effect of combining SRCi with the targeted inhibitor in HT29 (BRAF V600E mutation) cells. The simulations of the HT29 network predicted the combinatorial effect of SRCi and BRAFi that suppression of SRC activation induced by BRAFi, decreased activities of ERK and proliferation nodes, and effectively increased activity of apoptosis node (Figs. 4d and 6a). To test for the predicted synergistic reduction in viability, we exposed the cells to vemurafenib or AZ628 alone, dasatinib alone, or their combination for 5 days. We tested three concentrations of dasatinib. Although the lowest concentration of dasatinib was ineffective in reducing viability alone, when combined with either the AZ628 or the vemurafenib, viability was significantly reduced (Fig. 6b, c and Supplementary Fig. 5). Crystal violet assays and phase contrast images also showed the synergistic inhibition of cell viability (Fig. 6d). Western blot analysis of HT29 cells exposed to vemurafenib revealed a transient reduction in pERK within 1 h, followed by a rebound of its abundance after 24 h (Fig. 6e and Supplementary Fig. 6). Exposure to the SRCi alone or in combination with the BRAFi reduced pERK for the entire 48 h evaluated. In addition, combination treatment with dasatinib and vemurafenib increased early (PI^-, FITC-annexin V^+) and late (PI^+, FITC-annexin V^+) cell death in HT29 cells compared with those cells treated with BRAFi alone or SRCi alone (Fig. 6f, g). Taken together, single drug treatment of MAPK pathway inhibitors caused pathway reactivation and adaptive resistance in CRC cells with either KRAS or BRAF mutations, but combination treatment with SRCi suppressed adaptive resistance and increased the sensitivity of the cells to the cytotoxic effects of the MAPK inhibitors.

Targeting resistance-mediating hub node in feedback structure as combinatorial targets

Our simulations and experimental data with the CRC cells indicated that targeting resistance-mediating hub nodes, such as Src, may enhance the efficacy of drugs targeting molecules downstream within oncogenic signaling pathways by preventing adaptive resistance (Fig. 7a and Supplementary Fig. 7). The MAPK pathway is frequently altered many cancers [35, 36]. To determine if Src represented a resistance-mediating node in other cancers with mutations in the MAPK pathway, we tested the effects of the combination of an MAPK inhibitor and SRCi in lung cancer cell lines, SW1573 and A549, with KRAS mutations and in a triple negative breast cancer cell line, MDA-MB-231, with both KRAS and BRAF mutations (Supplementary Table 3). Although individually the MEKi and SRCi reduced cell viability, the combined treatment was more effective in reducing the viability of SW1573 (KRAS G12C) (Fig. 7b–d) and A549 (KRAS G12S) lung cancer cells (Supplementary Fig. 8). Similarly, combined treatment of MEKi or RAFi and SRCi synergistically impaired cell viability of MDA-MB-231 (KRAS G13D and BRAF G464V) triple negative breast cancer cells (Fig. 7e–g). These data with the lung cancer and breast cancer cells indicated that the combination of MAPK pathway inhibitors and SRCi might prevent adaptive resistance and exhibit benefit in cancer patients with MAPK pathway alterations. Although our signaling network was constructed for CRC, we tested the application of our approach for lung and breast cell lines by mapping the genomic information from CCLE database to our signaling network (Supplementary Fig. 9A). The scores calculated for MEKi and RAFi from the mapped networks generally predicted SRC as an effective combinatorial target, which are in agreement with the above experimental results, except for the A549 network (Supplementary Fig. 9B and Supplementary Data 5). Beyond our CRC signaling network, applying our approach to cancer type-specific networks may make more valuable predictions.

Src represents a regulatory node in other receptor tyrosine kinase pathways with positive feedback loops, in

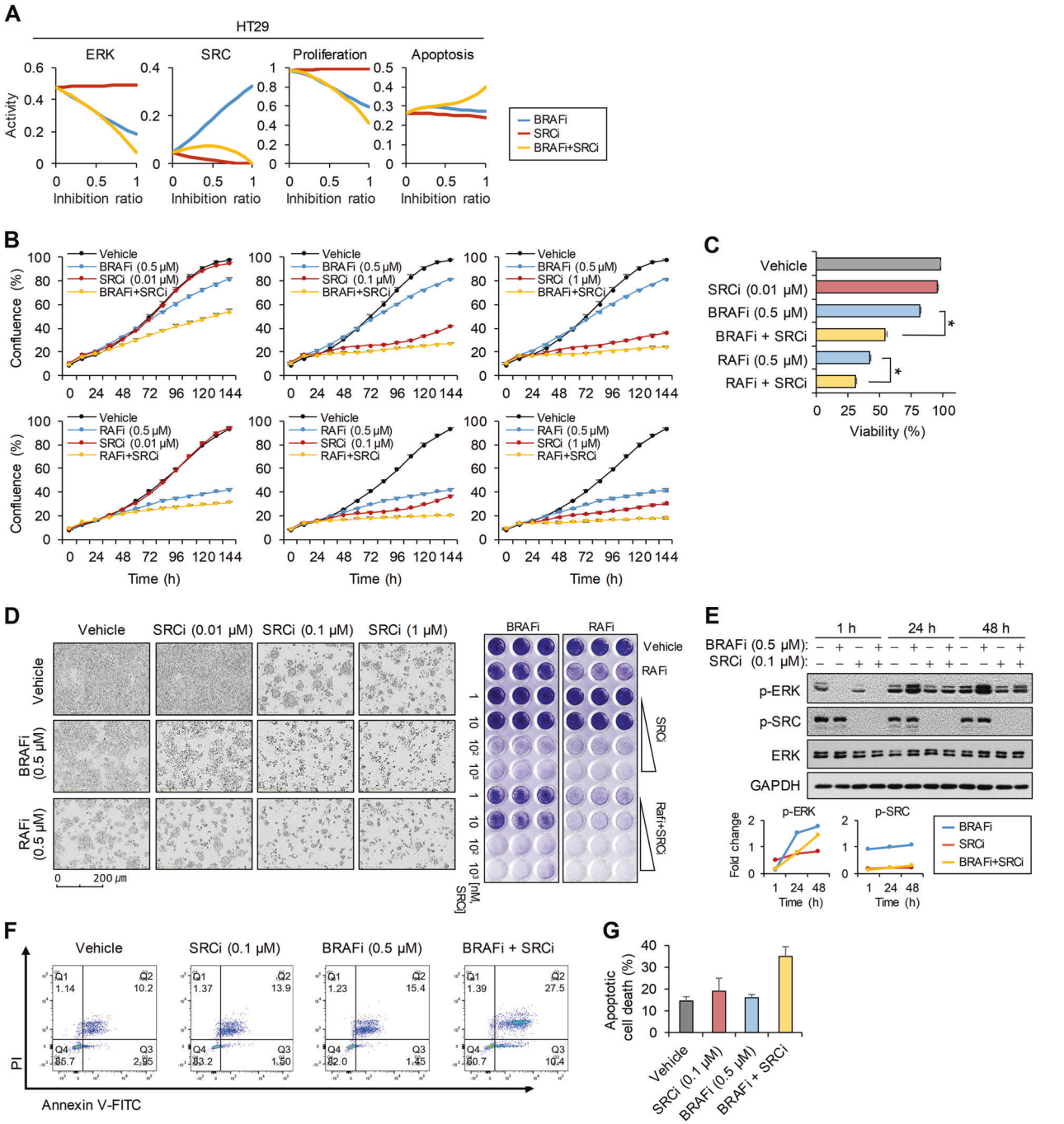

Fig. 6 Combination effect of SRCi and BRAFi in BRAF-mutant CRC cells. a Simulated drug response curves in the HT29 network. **b** Analysis of cell growth. HT29 cells were incubated for 24 h in 96-well plate (0.7×10^4 cells/well) and then treated with BRAFi (vemurafenib, 1 μM) or RAFi (AZ628, 1 μM) alone, SRCi (dasatinib, 0.01, 0.1, or 1 μM) alone, or in combination for 5 days. Cell growth was determined by cell confluence (%). **c** Analysis of cell viability. Cell viability was measured by using WST-1 assay after 5 days treatment with indicated drugs. The results are presented by means ± SEM (error bars) ($n = 3$). *$P < 0.05$ by two-sided Student's t test. **d** Images were taken 5 days after the indicated treatment (left). Crystal violet staining of colony growth treated with indicated drugs (right). **e** HT29 cells were subjected to the indicated treatments, then the indicated proteins were detected by Western blot. pERK is an indicator of adaptive resistance. pERK and p-SRC were quantified and normalized with GAPDH. Line graphs were plotted by fold change values normalized with vehicle at each time point. **f** Apoptotic cell death of HT29 cells. Cells were treated with the BRAFi (0.5 μM), SRCi (0.1 μM), and BRAFi plus SRCi for 48 h. Cells were stained with PI and Annexin V-FITC, and were analyzed by flow cytometry (Q4: live cells; Q3: early apoptotic cells; Q2: late apoptotic cells; Q1: necrotic cells). The acquisition of Annexin V-FITC and PI data is expressed as a percentage (%) in each quadrant. **g** The percentage of apoptotic cell death was examined by annexin V-FITC/PI staining and flow cytometry analysis. The results are presented as mean ± SD of two independent experiments.

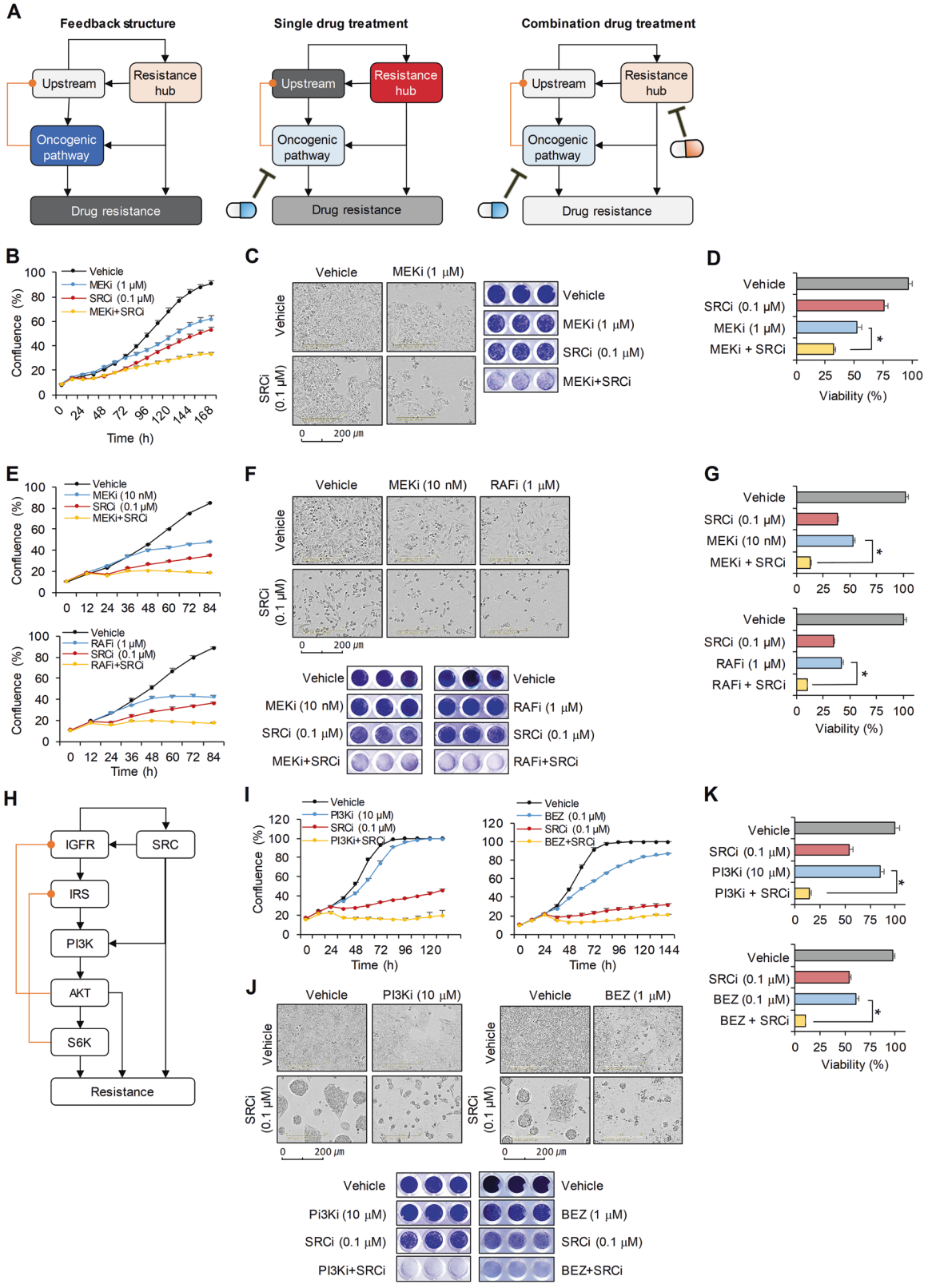

particular those that stimulate the PI3K pathway (Fig. 7h). Therefore, we investigated whether the proposed combinatorial treatment strategy model could be applied generally to signal networks with this structure. The PI3K pathway is another frequently mutated oncogenic pathway that is involved in cancer proliferation and survival [37], and

◀ **Fig. 7 Proposed generic model for the role of Src in adaptive resistance. a** The abstracted generic model for adaptive resistance in the signaling network (left). Adaptive resistance can emerge from targeting an oncogenic pathway (middle), and targeting a resistance hub can prevent resistance (right). **b** Analysis of cell growth. SW1573 cells were incubated for 24 h in 96-well plate (0.7×10^4 cells/well) and then treated with MEKi (trametinib, 1 μM) alone, SRCi (dasatinib, 0.1) alone, or in combination for 6 days. Cell growth was determined by cell confluence (%). **c** Images were taken 6 days after MEKi alone, SRCi alone, or in combination treatment (left). Crystal violet staining of colony growth treated with indicated drugs (right). **d** Analysis of cell viability. Cell viability was measured by using WST-1 assay after 6 days treatment with indicated drugs. **e** Analysis of cell growth. MDA-MB-231 cells were incubated for 24 h in 96-well plate (0.7×10^4 cells/well) and then treated with MEKi (trametinib, 0.01 μM) or RAFi (AZ628, 1 μM) alone, SRCi (dasatinib, 0.1 μM) alone, or in combination for 60 h. Cell growth was determined by cell confluence (%). **f** Images were taken 60 h after MEKi alone, SRCi alone, or in combination treatment (top). Crystal violet staining of colony growth treated with indicated drugs (bottom). **g** Analysis of cell viability. Cell viability was measured by using WST-1 assay after 60 h treatment with indicated drugs. **h** The network model for adaptive resistance in the PI3K pathway with regulatory input from SRC. **i** Analysis of cell growth. HCT116 cells were incubated for 24 h in 96-well plate (0.7×10^4 cells/well) and then treated with PI3Ki (BYL719, 1 μM) or BEZ (NVP-BEZ235, 0.1 μM) alone, SRCi (dasatinib, 0.1 μM) alone, or in combination for 5 days. Cell growth was determined by cell confluence (%). **j** Images were taken 5 days after the indicated treatment (top). Crystal violet staining of colony growth treated with indicated drugs (bottom). **k** Analysis of cell viability. Cell viability was measured by using WST-1 assay after 5 days treatment with indicated drugs. The results are presented by means ± SEM (error bars) ($n = 3$). $^*P < 0.05$ by two-sided Student's t test.

various cancer drugs target this pathway [38]. Similar to the MAPK pathway, Src interacts with the PI3K pathway with upstream and downstream nodes and represent a bypass pathway in our network model (Fig. 7h and Supplementary Fig. 10A). Therefore, this network can be abstracted with the same feedback structure as in Fig. 7a.

To investigate the combination of PI3K pathway inhibitor and SRCi, we treated HCT116 cells, which have both a KRAS mutation and a PI3K mutation, with the PI3Kα inhibitor BYL719 or the PI3K and mechanistic target of rapamycin (mTOR) inhibitor BEZ235, the SRCi dasatinib, or their combination for 6 days and monitored viability (Fig. 7i–k). Like the combination of SRCi and MAPK inhibitor, the combination of PI3K pathway inhibitors and SRCi synergistically reduced viability (Fig. 7i, k) and induced death of HCT116 cells (Fig. 7j). The scores calculated for PI3K inhibitor (PI3Ki) from the HCT116 network also predicted SRC as the most effective combinatorial target (Supplementary Fig. 10B and Supplementary Data 5). These results indicated that combinatorial targeting of the resistance-mediating hub in the oncogenic pathway networks with such a feedback and regulatory structure may be an effective mechanism to overcome resistance to drugs targeting the oncogenic pathway.

Discussion

Cancer is caused by the accumulation of genetic alterations resulting in a rewired signaling network that maintains cancerous growth and survival [39, 40]. Molecular-targeted therapy aims to disturb the cancer signaling network by inhibiting specific drug targets, such as signaling molecules in the oncogenic network [41]. Most targeted drugs inhibit the oncogene or oncogenic pathway that drove tumorigenesis [42]. However, emergence of resistance in cancer is a substantial barrier to long-term effectiveness of cancer treatment with targeted drugs [1]. In the signaling network of cancer cells, negative feedback regulatory loops from downstream to upstream of a pathway and crosstalk links between pathways maintain cellular homeostasis [3]. Thus, inhibition of the target can relieve negative feedback from the drug target and activate upstream signaling in the targeted pathway, resulting in reactivation of the targeted pathway or compensatory activation of bypass signaling pathways [2, 43]. Collectively or individually, these events cause adaptive resistance and are often induced by drugs targeting various pathways. Consequently, adaptive resistance is common in targeted cancer therapy. Therefore, it is necessary to establish new strategies to maximize the therapeutic efficacy and prevent adaptive resistance. Here, we developed a probabilistic Boolean simulation framework to analyze adaptive resistance in a signaling network and to identify combinatorial targets for overcoming the resistance. The model simulations predicted Src as a key combinatorial target, and we experimentally demonstrated that co-inhibition of Src increased sensitivity of CRC cells to the cytotoxicity of either MAPK-targeted or PI3K-targeted inhibitors.

Systems approaches combined with computational methods have revealed underlying mechanisms of complex biological phenomena [44–54], including how adaptive drug resistance occurs in cancer [55, 56]. Such analyses were usually performed with ODE models, but analysis of signaling networks with ODE models is limited by the scale of the network, because ODE models require fitting all the kinetic parameter values to time-series experimental measurements [17–19]. Thus, previous studies of adaptive resistance to drugs using ODE models mainly focused on small-scale networks that included a few pathways. In contrast to ODE models, analysis of signaling networks with a Boolean model is extendable to large-scale networks, because Boolean models are parameter free, as well as computationally tractable because they incorporate the discrete state of a node and the logical relationship between nodes. However, we showed that the deterministic drug simulation of previous cancer studies is not suitable for the analysis of the dynamics of networks with feedback regulation. Instead, we developed a probabilistic Boolean

framework and demonstrated that the dynamics of such complex networks can be captured by this framework.

We selected to evaluate adaptive resistance to drugs targeting the MAPK pathway, because such drugs are used clinically and resistance is common. We computationally identified Src as a combinatorial target. Src is a nonreceptor tyrosine kinase with regulatory inputs into several signaling pathways, including the EGFR, IGFR, and JAK/STAT pathways. Src has been investigated as a molecular target for cancer therapy, because the abundance and activity of Src increase during CRC progression [57]. However, single treatment with SRCi in CRC failed to produce the promising results in clinical trials [58]. Further studies sought an effective combinatorial drug for SRCi targeting an upstream receptor [58]. Although combined treatment of SRCi with EGFRi was effective in CRC cells [59], this combination showed little clinical activity in CRC patients [60]. Here, we identified Src as an effective combination target with MAPK pathway inhibitors. We also demonstrated experimentally that combining SRCi with BRAFi or MEKi in KRAS- or BRAF-mutant CRC cells produced a synergistic reduction on cell viability. Our findings with MEKi and SRCi are consistent with a previous study of KRAS-mutant CRC cells [61]. Unlike the previous study, which identified Src by extensive screening experiments using CRISPR/Cas9, we found Src as a combination target through systems analysis of a network model using simulations. Thus, our approach avoids the need for extensive experiments.

We note the assumption behind the presented method and the resulting limitations. In our scoring measure for selecting combinatorial targets, we assumed the pathway distance as a negative factor since we considered the activity changes of the nodes in shorter distances would have greater effects on a target node compared with those distant nodes the effects of which on the target node might be compensated or interrupted during their longer signal transduction by signals from different paths in the whole signaling network where crosstalks and feedback regulations result in complicated wiring. However, in some cases, a signaling pathway can amplify signals through signal transduction and this may result in unexpected consequences on influencing the target node. Our approach may not identify such distant but actually effective node whose signaling is not diluted along the pathway, which is the limitation of the presented method.

Traditional clinical trials in oncology have tested a drug effect in specific cancer type [62]. Basket trials test a drug effect in patients with a specific genomic profile regardless of their cancer types [62]. Similar to the strategy of targeting therapy on the basis of genomic profile, our study suggested that a common drug combination strategy can be applied to patients with genetic alterations within the MAPK signaling pathway. We showed that combined treatment of SRCi and MAPK pathway inhibitors is effective in CRC, lung, and breast cancer cells. The combination of SRCi is effective with BRAFi in BRAF-mutant melanoma [63] or with RAFi in BRAF- or NRAS-mutant melanoma and that combining SRCi with RAFi prevents pathway reactivation [64]. Our data and the previous results support that hypothesis that Src is an effective combinatorial target for MAPK pathway inhibitors in various cancer types. Many cancers have multiple cancer-driving mutations. Indeed, HCT116 cells have mutations in both the MAPK pathway and the PI3K pathway. Importantly, we showed that combined treatment of SRCi and PI3K pathway inhibitors is also effective in reducing CRC cell viability in cells with activating mutations in both the MAPK and PI3K pathway. Taken together, our data indicated that Src has a pivotal role in drug resistance to multiple pathways, particularly for MAPK and PI3K pathways, in a wide range of cancer types.

An advantage of our approach is that it is generalizable. By developing a PBN and applying probabilistic simulations, we demonstrated that such an approach can identify resistance-mediating nodes in a complex network with NFLs and interpathway connections. Furthermore, we generated a large-scale signaling network representing pathways important in controlling cancer cell proliferation, survival, and apoptosis and integrated genomic information into the PBN to produce networks specific to a cancer's genetic profile. Although here we applied our framework to CRC and identified Src as an effective combination target with MAPK inhibitors and PI3Ki, this approach can be widely used to discover critical combinatorial therapeutic strategies to overcome the commonly observed adaptive resistance in cancer.

Methods

Drug simulation framework using probabilistic Boolean modeling

Protein activity is actually a continuous value measured by amounts of phosphorylated form or expression levels of a protein. However, a Boolean model represents the state of a node (i.e. protein activity) in a binary fashion as 0 or 1 to simplify the computational complexity. To overcome such a limitation, various previous studies using Boolean models estimated a node activity by measuring the average ON state of nodes over repeated simulations [65–68]. By adopting such an approach in our simulation framework, we could quantitatively interpret an intermediate activity of nodes.

The state of a node targeted by a drug was probabilistically updated according to one of two truth tables: either

a table containing original logical dynamics or a table representing drug inhibition in which all the output states of the table are OFF (Supplementary Fig. 1). The inhibition ratio of a drug target node, ranging from 0 to 1, determined the probability that the node updates its state following the table for inhibitory logic; otherwise, the node updates its state following the table for original logic. After 10,000 simulation steps of probabilistic drug perturbation with an inhibition ratio, the activity of each node was calculated by the average of state values during the simulation. The drug effect was measured by AUC of the response curve indicating the change of activity with the change of inhibition ratio.

After drug treatment to a node within NFLs, its downstream node can be reactivated over time such that the node activity is transiently inhibited and then increased similarly to its initial activity level as illustrated in Fig. 1b. However, analysis of time-dependent changes is limited in Boolean models, which mainly concern steady-state dynamics. Therefore, we focused the steady-state phenomena caused by the reactivation mechanism, which is drug resistance in NFLs.

Construction of the signaling network

We reconstructed a Boolean model for a signaling network of CRC by integrating the published literature and information from public databases. The resulting network consisted of 95 nodes and 341 links as provided in Supplementary Data 1: source denoted upstream nodes that are molecules regulating target nodes; target denoted downstream nodes that are molecules regulated by source nodes; link type denoted regulations between source and target nodes as "+" for an activatory link and "−" for an inhibitory link; logic equation denoted logical functions of target nodes that were determined by mechanistic information of the relevant literature. When information about detailed regulation relationship was limited, we formulated the logical function of a node with multiple inputs using OR gates for activatory links and AND gates for inhibitory links [69]. The basal activity of the EGF input node was set to 0.5 throughout drug simulations.

Score for selecting combinatorial targets

The AC measured adaptive effects of node activity by drugs. In the response curve of nodes obtained from drug simulations, the AC of each node was calculated by AUC above the node activity prior to drug administration.

In a signaling network, competition between signaling molecules occurs when multiple downstream molecules are regulated by a common upstream molecule. If one downstream molecule is fully regulated by an upstream molecule, others are less regulated due to the limited binding capacity. In consequence, the signaling effect can be diluted along different pathways, resulting in attenuation depend on the length of a pathway. To adjust distance effects of feedback loops in adaptive responses, we divided AC by the length of shortest NFL (LN) between each node and ERK in the nominal network (Supplementary Fig. 11).

Bypass signaling effects from each node to output nodes, apoptosis (BA) and proliferation (BP), were calculated in the nominal network considering distance effects of bypass paths as follows:

$$\mathrm{BP} = \sum_{k=1}^{l} \frac{1}{L_{\mathrm{P}}^{+}(k)} - \sum_{k=1}^{l} \frac{1}{L_{\mathrm{P}}^{-}(k)},$$

$$\mathrm{BA} = \sum_{k=1}^{l} \frac{1}{L_{\mathrm{A}}^{+}(k)} - \sum_{k=1}^{l} \frac{1}{L_{\mathrm{A}}^{-}(k)},$$

where L_{A} or L_{P} denotes the set of lengths of every path from each node to apoptosis or proliferation node, respectively. L^{+} or L^{-} includes the lengths of activatory or inhibitory paths to the corresponding output node, respectively. $L(k)$ denotes the path lengths of k. Among the paths whose lengths were in the range of 1 to l, we calculated the bypass signaling effect by subtracting the sum of the inverted lengths of all activatory pathways from the sum of the inverted lengths of all inhibitory pathways (Supplementary Fig. 11). Since the characteristic path length of the CRC signaling network was calculated as 3.989, which is the average shortest path length between nodes, we used a large value of $l = 8$ as the maximum path length to consider. Consequently, a node enriched with short activatory paths to output nodes gets a high value for bypass signaling effects.

Finally, the score was calculated as follow:

$$\mathrm{Score} = \frac{\mathrm{AC} \cdot \theta(\mathrm{AC})}{\mathrm{LN}} \cdot (\mathrm{BP} - \mathrm{BA}),$$

where θ denotes Heaviside step function whose value is 0 or 1 for negative or positive arguments, respectively. We multiplied θ(AC) to consider a node with only positive AC as a candidate of a combination target. Thereby, nodes showing high AC in the positive direction, connected by short LN, and transmitting more positive BP and more negative BA can get high scores.

Cell culture

HT29 (BRAF V600E and PI3K P449T) and SW1573 (KRAS G12C) cells were obtained from the American Type Culture Collection (ATCC). HCT116 (KRAS G13D and PI3K H1047R), SW620 (KRAS G12V), A549 (KRAS G12S), and MDA-MB-231 (KRAS G13D and BRAF G464V) cells were obtained from Korean Cell Line Bank.

All cell lines were cultured in Dulbecco's modified Eagle's medium (WelGENE Inc., Gyeongsan, Republic of Korea) with 10% fetal bovine serum (FBS, WelGENE Inc.) and antibiotics (100 U/ml of penicillin, 100 μg/ml streptomycin, and 0.25 μg/ml of Fungizone) (Life Technologies Corp., Carlsbad, CA) at 37 °C in a humidified atmosphere containing 5% CO_2.

Reagents

Trametinib (GSK1120212, MEK1/2 inhibitor) was purchased from APExBIO (Boston, MA, USA). AZ628 (pan-Raf inhibitor), dasatinib (SRCi), vemurafenib (PLX4032, B-Raf^{V600E} inhibitor), alpelisib (BYL719, PI3Kα inhibitor), and dactolisib (NVP-BEZ235, PI3K, and mTOR inhibitor) were obtained from Selleckchem (Houston, TX, USA). Crystal violet solution, dimethyl sulfoxide (DMSO), and paraformaldehyde (PFA) were obtained from Sigma-Aldrich (Saint Louis, MO, USA).

Cell growth and viability assays

Cells were seeded into 96-well plate at a density of 3–7 × 10^3 cells/well in growth medium, incubated for 24 h and then treated with the indicated drugs. Following incubation of the plates for 72–120 h, relative cell viability was measured. After seeding, cells were imaged using IncuCyte ZOOM. To assess cell growth, average areas of cells were determined at each time point using the IncuCyte ZOOM analysis software. Images were captured at 3 h intervals from three separate regions per well with a 20× objective. Relative cell viability was measured with WST-1 solution (Daeillab, Republic of Korea) by measuring absorbance at 450 nm using an xMark™ Microplate Absorbance Spectrophotometer (Bio-Rad, Hercules, CA).

Cristal violet assay

Cells were seeded at 3–7 × 10^3 cells/well. The next day, cells were treated with the indicated drugs and doses. Cells were incubated for 3–7 days after drug addition, plates were rinsed with PBS, fixed, and then stained with 0.5% (w/v) crystal violet (Sigma-Aldrich) for 30 min at room temperature. Plates were rinsed with tap water, dried, and photographed the next day.

Western blot analysis

Cells were lysed in lysis buffer (20 mM HEPES, pH 7.2, 150 mM NaCl, 0.5% Triton X-100, 10% glycerol, 1 μg/ml aprotinin, 1 μg leupeptin, 1 mM Na_3VO_4, 1 mM NaF). For immunoblotting, anti-ERK1/2 (#9102), anti-phospho-ERK1/2 (#4370), anti-phospho-Src (#6943, Cell Signaling Technology, Inc., Danvers, MA), and anti-β-actin (sc-1616, Santa Cruz Biotechnology, Inc., Dallas, TX) were used. The rabbit polyclonal anti-GAPDH antibody was a generous gift from Dr Ki-Sun Kwon (Korea Research Institute of Bioscience and Biotechnology). The protein bands were quantified in ImageJ (NIH, Bethesda, MD).

Measuring apoptosis using flow cytometry

Apoptosis was analyzed by Annexin V-FITC/PI apoptosis detection kit (abcam, Cambridge, UK) using flow cytometry (FACSAria II, BD Biosciences, San Jose, CA). Briefly, HCT116 and HT29 cells (1 × 106 cells) were seeded into 10 cm dish and treated with indicated drugs for 48 h. And then, cells were harvested, washed with PBS, resuspended in 1× binding buffer, labeled with FITC conjugated Annexin V and PI, and acquired on FACSAria II flow cytometry (BD Biosciences) using the FACSDIVA™ software (BD Biosciences). At the end, percentages of apoptotic cells were calculated using FlowJo™ software (Version 10.6.1, BD Biosciences).

Statistical analysis

Statistical analysis was performed using two-sided Student's t test. Differences were statistical significant at $P < 0.05$. All experiments were repeated at least three times, and data were shown as the mean ± SEM.

Code availability

All codes are available from the authors upon request.

Acknowledgements We thank Dr Ki-Sun Kwon (Korea Research Institute of Bioscience and Biotechnology) for the rabbit polyclonal anti-GAPDH antibody, Nancy R. Gough (BioSerendipity, LLC) for editorial assistance, and Sea Choi for her editorial assistance during revision. This work was supported by the National Research Foundation of Korea (NRF) grants funded by the Korea Government, the Ministry of Science and ICT (2017R1A2A1A17069642 and 2015M3A9A7067220).

Author contributions K-HC, S-MP, and CYH conceived the study and designed computational simulations and experiments. S-MP conducted modeling and analysis. CYH performed experiments. JC provided experimental support, and CYJ provided analytical support. S-MP, CYH and K-HC wrote the paper. K-HC designed the project and supervised the study.

Compliance with ethical standards

Conflict of interest The authors declare that they have no conflict of interest.

Publisher's note Springer Nature remains neutral with regard to jurisdictional claims in published maps and institutional affiliations.

References

1. Garraway LA, Janne PA. Circumventing cancer drug resistance in the era of personalized medicine. Cancer Discov. 2012;2:214–26.
2. Chen SH, Lahav G. Two is better than one; toward a rational design of combinatorial therapy. Curr Opin Struct Biol. 2016;41:145–50.
3. Sun C, Bernards R. Feedback and redundancy in receptor tyrosine kinase signaling: relevance to cancer therapies. Trends Biochem Sci. 2014;39:465–74.
4. Duncan JS, Whittle MC, Nakamura K, Abell AN, Midland AA, Zawistowski JS, et al. Dynamic reprogramming of the kinome in response to targeted MEK inhibition in triple-negative breast cancer. Cell. 2012;149:307–21.
5. Johnson GL, Stuhlmiller TJ, Angus SP, Zawistowski JS, Graves LM. Molecular pathways: adaptive kinome reprogramming in response to targeted inhibition of the BRAF-MEK-ERK pathway in cancer. Clin Cancer Res. 2014;20:2516–22.
6. Lito P, Rosen N, Solit DB. Tumor adaptation and resistance to RAF inhibitors. Nat Med. 2013;19:1401–9.
7. Kopetz S, Desai J, Chan E, Hecht JR, O'Dwyer PJ, Lee RJ, et al. PLX4032 in metastatic colorectal cancer patients with mutant BRAF tumors. J Clin Oncol. 2010;28:3534.
8. Prahallad A, Sun C, Huang S, Di Nicolantonio F, Salazar R, Zecchin D, et al. Unresponsiveness of colon cancer to BRAF (V600E) inhibition through feedback activation of EGFR. Nature. 2012;483:100–3.
9. Corcoran RB, Ebi H, Turke AB, Coffee EM, Nishino M, Cogdill AP, et al. EGFR-mediated re-activation of MAPK signaling contributes to insensitivity of BRAF mutant colorectal cancers to RAF inhibition with vemurafenib. Cancer Discov. 2012;2:227–35.
10. Lamba S, Russo M, Sun C, Lazzari L, Cancelliere C, Grernrum W, et al. RAF suppression synergizes with MEK inhibition in KRAS mutant cancer cells. Cell Rep. 2014;8:1475–83.
11. Kolch W, Halasz M, Granovskaya M, Kholodenko BN. The dynamic control of signal transduction networks in cancer cells. Nat Rev Cancer. 2015;15:515–27.
12. Assmus HE, Herwig R, Cho KH, Wolkenhauer O. Dynamics of biological systems: role of systems biology in medical research. Expert Rev Mol Diagn. 2006;6:891–902.
13. Sreenath SN, Cho KH, Wellstead P. Modelling the dynamics of signalling pathways. Essays Biochem. 2008;45:1–28.
14. Park SM, Hwang CY, Cho SH, Lee D, Gong JR, Lee S, et al. Systems analysis identifies potential target genes to overcome cetuximab resistance in colorectal cancer cells. FEBS J. 2019;286:1305–18.
15. Choi M, Shi J, Zhu Y, Yang R, Cho KH. Network dynamics-based cancer panel stratification for systemic prediction of anticancer drug response. Nat Commun. 2017;8:1940.
16. Gomez Tejeda Zanudo J, Scaltriti M, Albert R. A network modeling approach to elucidate drug resistance mechanisms and predict combinatorial drug treatments in breast cancer. Cancer Converg. 2017;1:5.
17. Aldridge BB, Burke JM, Lauffenburger DA, Sorger PK. Physicochemical modelling of cell signalling pathways. Nat Cell Biol. 2006;8:1195–203.
18. Saez-Rodriguez J, Alexopoulos LG, Epperlein J, Samaga R, Lauffenburger DA, Klamt S, et al. Discrete logic modelling as a means to link protein signalling networks with functional analysis of mammalian signal transduction. Mol Syst Biol. 2009;5:331.
19. Kim J, Park S-M, Cho K-H. Discovery of a kernel for controlling biomolecular regulatory networks. Sci Rep. 2013;3:2223.
20. Corcoran RB, Atreya CE, Falchook GS, Kwak EL, Ryan DP, Bendell JC, et al. Combined BRAF and MEK inhibition with dabrafenib and trametinib in BRAF V600-mutant colorectal cancer. J Clin Oncol. 2015;33:4023–31.
21. Shmulevich I, Dougherty ER, Kim S, Zhang W. Probabilistic Boolean networks: a rule-based uncertainty model for gene regulatory networks. Bioinformatics. 2002;18:261–74.
22. Kanehisa M, Goto S. KEGG: kyoto encyclopedia of genes and genomes. Nucleic Acids Res. 2000;28:27–30.
23. Schaefer CF, Anthony K, Krupa S, Buchoff J, Day M, Hannay T, et al. PID: the pathway interaction database. Nucleic Acids Res. 2009;37:D674–9.
24. Cancer Genome Atlas N. Comprehensive molecular characterization of human colon and rectal cancer. Nature. 2012; 487:330–7.
25. Fearon ER. Molecular genetics of colorectal cancer. Annu Rev Pathol. 2011;6:479–507.
26. Wee P, Wang Z. Epidermal growth factor receptor cell proliferation signaling pathways. Cancers. 2017;9:1–15.
27. He G, Siddik ZH, Huang Z, Wang R, Koomen J, Kobayashi R, et al. Induction of p21 by p53 following DNA damage inhibits both Cdk4 and Cdk2 activities. Oncogene. 2005;24:2929–43.
28. Jeong WJ, Ro EJ, Choi KY. Interaction between Wnt/beta-catenin and RAS-ERK pathways and an anti-cancer strategy via degradations of beta-catenin and RAS by targeting the Wnt/beta-catenin pathway. NPJ Precis Oncol. 2018;2:5.
29. Ikushima H, Miyazono K. TGFbeta signalling: a complex web in cancer progression. Nat Rev Cancer. 2010;10:415–24.
30. Barretina J, Caponigro G, Stransky N, Venkatesan K, Margolin AA, Kim S, et al. The Cancer Cell Line Encyclopedia enables predictive modelling of anticancer drug sensitivity. Nature. 2012;483:603–7.
31. Chakravarty D, Gao J, Phillips SM, Kundra R, Zhang H, Wang J, et al. OncoKB: a precision oncology knowledge base. JCO Precis Oncol. 2017;1:1–16.
32. Thieffry D, Romero D. The modularity of biological regulatory networks. Biosystems. 1999;50:49–59.
33. Klinger B, Sieber A, Fritsche-Guenther R, Witzel F, Berry L, Schumacher D, et al. Network quantification of EGFR signaling unveils potential for targeted combination therapy. Mol Syst Biol. 2013;9:673.
34. Turke AB, Song Y, Costa C, Cook R, Arteaga CL, Asara JM, et al. MEK inhibition leads to PI3K/AKT activation by relieving a negative feedback on ERBB receptors. Cancer Res. 2012; 72:3228–37.
35. Dhillon AS, Hagan S, Rath O, Kolch W. MAP kinase signalling pathways in cancer. Oncogene. 2007;26:3279–90.
36. Imperial R, Toor OM, Hussain A, Subramanian J, Masood A. Comprehensive pancancer genomic analysis reveals (RTK)-RAS-RAF-MEK as a key dysregulated pathway in cancer: its clinical implications. Semin Cancer Biol. 2019;54:14–28.
37. Danielsen SA, Eide PW, Nesbakken A, Guren T, Leithe E, Lothe RA. Portrait of the PI3K/AKT pathway in colorectal cancer. Biochim Biophys Acta. 2015;1855:104–21.
38. Courtney KD, Corcoran RB, Engelman JA. The PI3K pathway as drug target in human cancer. J Clin Oncol. 2010;28:1075–83.
39. Shin D, Lee J, Gong JR, Cho KH. Percolation transition of cooperative mutational effects in colorectal tumorigenesis. Nat Commun. 2017;8:1270.
40. Creixell P, Schoof EM, Simpson CD, Longden J, Miller CJ, Lou HJ, et al. Kinome-wide decoding of network-attacking mutations rewiring cancer signaling. Cell. 2015;163:202–17.
41. Sawyers C. Targeted cancer therapy. Nature. 2004;432:294–7.
42. Sharma SV, Settleman J. Oncogene addiction: setting the stage for molecularly targeted cancer therapy. Genes Dev. 2007; 21:3214–31.

43. Konieczkowski DJ, Johannessen CM, Garraway LA. A convergence-based framework for cancer drug resistance. Cancer Cell. 2018;33:801–15.
44. Murray PJ, Kang JW, Mirams GR, Shin SY, Byrne HM, Maini PK, et al. Modelling spatially regulated beta-catenin dynamics and invasion in intestinal crypts. Biophys J. 2010;99:716–25.
45. Schmidt H, Cho KH, Jacobsen EW. Identification of small scale biochemical networks based on general type system perturbations. FEBS J. 2005;272:2141–51.
46. Sontag ED. Network reconstruction based on steady-state data. Essays Biochem. 2008;45:161–76.
47. Eshaghi M, Lee JH, Zhu L, Poon SY, Li J, Cho K-H, et al. Genomic binding profiling of the fission yeast stress-activated MAPK Sty1 and the bZIP transcriptional activator Atf1 in response to H2O2. PloS One. 2010;5:e11620.
48. Kim S, Kim J, Cho K-H. Inferring gene regulatory networks from temporal expression profiles under time-delay and noise. Comput Biol Chem. 2007;31:239–45.
49. Kwon Y-K, Cho K-H. Analysis of feedback loops and robustness in network evolution based on Boolean models. BMC Bioinform. 2007;8:430.
50. Kwon Y-K, Cho K-H. Boolean dynamics of biological networks with multiple coupled feedback loops. Biophys J. 2007;92:2975–81.
51. Park SG, Lee T, Kang HY, Park K, Cho K-H, Jung G. The influence of the signal dynamics of activated form of IKK on NF-κB and anti-apoptotic gene expressions: a systems biology approach. FEBS Lett. 2006;580:822–30.
52. Murray PJ, Kang J-W, Mirams GR, Shin S-Y, Byrne HM, Maini PK, et al. Modelling spatially regulated β-catenin dynamics and invasion in intestinal crypts. Biophys J. 2010;99:716–25.
53. Kim J-R, Cho K-H. The multi-step phosphorelay mechanism of unorthodox two-component systems in *E. coli* realizes ultra-sensitivity to stimuli while maintaining robustness to noises. Comput Biol Chem. 2006;30:438–44.
54. Kim J-R, Kim J, Kwon Y-K, Lee H-Y, Heslop-Harrison P, Cho K-H. Reduction of complex signaling networks to a representative kernel. Sci Signal. 2011;4:ra35.
55. Sturm OE, Orton R, Grindlay J, Birtwistle M, Vyshemirsky V, Gilbert D, et al. The mammalian MAPK/ERK pathway exhibits properties of a negative feedback amplifier. Sci Signal. 2010;3:ra90.
56. Kirouac DC, Schaefer G, Chan J, Merchant M, Orr C, Huang SA, et al. Clinical responses to ERK inhibition in BRAF(V600E)-mutant colorectal cancer predicted using a computational model. NPJ Syst Biol Appl. 2017;3:14.
57. Yeatman TJ. A renaissance for SRC. Nat Rev Cancer. 2004; 4:470–80.
58. Gargalionis AN, Karamouzis MV, Papavassiliou AG. The molecular rationale of Src inhibition in colorectal carcinomas. Int J Cancer. 2014;134:2019–29.
59. Dunn EF, Iida M, Myers RA, Campbell DA, Hintz KA, Armstrong EA, et al. Dasatinib sensitizes KRAS mutant colorectal tumors to cetuximab. Oncogene. 2011;30:561–74.
60. Parseghian CM, Parikh NU, Wu JY, Jiang ZQ, Henderson L, Tian F, et al. Dual inhibition of EGFR and c-Src by cetuximab and dasatinib combined with FOLFOX chemotherapy in patients with metastatic colorectal cancer. Clin Cancer Res. 2017;23:4146–54.
61. Anderson GR, Winter PS, Lin KH, Nussbaum DP, Cakir M, Stein EM, et al. A landscape of therapeutic cooperativity in KRAS mutant cancers reveals principles for controlling tumor evolution. Cell Rep. 2017;20:999–1015.
62. Ornes S. Core concept: basket trial approach capitalizes on the molecular mechanisms of tumors. Proc Natl Acad Sci USA. 2016;113:7007–8.
63. Girotti MR, Pedersen M, Sanchez-Laorden B, Viros A, Turajlic S, Niculescu-Duvaz D, et al. Inhibiting EGF receptor or SRC family kinase signaling overcomes BRAF inhibitor resistance in melanoma. Cancer Discov. 2013;3:158–67.
64. Girotti MR, Lopes F, Preece N, Niculescu-Duvaz D, Zambon A, Davies L, et al. Paradox-breaking RAF inhibitors that also target SRC are effective in drug-resistant BRAF mutant melanoma. Cancer Cell. 2015;27:85–96.
65. Helikar T, Konvalina J, Heidel J, Rogers JA. Emergent decision-making in biological signal transduction networks. Proc Natl Acad Sci USA. 2008;105:1913–8.
66. Lee HS, Goh MJ, Kim J, Choi TJ, Kwang Lee H, Joo Na Y, et al. A systems-biological study on the identification of safe and effective molecular targets for the reduction of ultraviolet B-induced skin pigmentation. Sci Rep. 2015;5:10305.
67. Park D, Lee HS, Kang JH, Kim SM, Gong JR, Cho KH. Attractor landscape analysis of the cardiac signaling network reveals mechanism-based therapeutic strategies for heart failure. J Mol Cell Biol. 2018;10:180–94.
68. Cho SH, Park SM, Lee HS, Lee HY, Cho KH. Attractor landscape analysis of colorectal tumorigenesis and its reversion. BMC Syst Biol. 2016;10:96.
69. Abdi A, Tahoori MB, Emamian ES. Fault diagnosis engineering of digital circuits can identify vulnerable molecules in complex cellular pathways. Sci Signal. 2008;1:ra10.